Rebound in Atmospheric Predictability and the Role of the Land Surface

ZHICHANG GUO

Center for Ocean–Land–Atmosphere Studies, Calverton, Maryland

PAUL A. DIRMEYER AND TIMOTHY DELSOLE

George Mason University, Fairfax, Virginia, and Center for Ocean–Land–Atmosphere Studies, Calverton, Maryland

RANDAL D. KOSTER

Global Modeling and Assimilation Office, NASA Goddard Space Flight Center, Greenbelt, Maryland

(Manuscript received 5 November 2011, in final form 1 March 2012)

ABSTRACT

Total predictability within a chaotic system like the earth's climate cannot increase over time. However, it can be transferred between subsystems. Predictability of air temperature and precipitation in numerical model forecasts over North America rebounds during late spring to summer because of information stored in the land surface. Specifically, soil moisture anomalies can persist over several months, but this memory cannot affect the atmosphere during early spring because of a lack of coupling between land and atmosphere. Coupling becomes established in late spring, enabling the effects of soil moisture anomalies to increase atmospheric predictability in 2-month forecasts begun as early as 1 May. This predictability is maintained through summer and then drops as coupling fades again in fall. This finding suggests summer forecasts of rainfall and air temperature over parts of North America could be significantly improved with soil moisture observations during spring.

1. Introduction

The atmosphere is a chaotic system where nonlinearities and instabilities cause small uncertainties in the initial state to grow exponentially in time. This error growth and the nature of the current observing system limit useful deterministic weather predictions to roughly 2 weeks (Shukla 1981; Simmons and Hollingsworth 2002). Any useful atmospheric predictability beyond 2 weeks must arise from interactions with the more slowly varying parts of the climate system, such as the ocean, land, sea ice, or snow cover, or from predictable external forcing. On seasonal time scales, atmospheric variability due to external radiative forcing is believed to be negligible, whereas variability due to interactions with the ocean and land is well established (Shukla and Kinter 2006).

According to information theory, the total predictability of any stochastic (Markov) system decays monotonically with time (Cover and Thomas 1991). Thus, the predictability of the entire climate system decreases with the length of forecast. However, this theorem pertains to the system as a whole, not to individual components. Can the predictability within one component of the earth's climate system, such as the atmosphere or ocean, increase with forecast lead time? Such behavior is sometimes called ''return of skill'' or ''rebound in predictability'' (Anderson and Van den Dool 1994; Alexander et al. 1999; Wajsowicz 2007).

Previous studies of weather predictions have identified individual forecasts in which prediction skill increases with lead time, but these appear to be statistically insignificant random variations, in the sense that they occur as often as expected compared to chance (Anderson and Van den Dool 1994; Kleeman 2007). Technically, any variable with an oscillatory autocorrelation function could be said to exhibit rebound in predictability, because the square of the autocorrelation periodically increases and most predictability measures are monotonically

Corresponding author address: Zhichang Guo, Center for Ocean–Land–Atmosphere Studies, 4041 Powder Mill Road, Suite 302, Calverton, MD 20705.
E-mail: guo@cola.iges.org

DOI: 10.1175/JCLI-D-11-00651.1

© 2012 American Meteorological Society

related to the square of the autocorrelation function (DelSole and Tippett 2007). Such oscillatory autocorrelation functions are known to occur in the tropical Pacific Ocean and have been explained as coupled atmosphere–ocean interactions associated with the El Niño–Southern Oscillation phenomenon (Philander 1990). Similar features have been found in the tropical Indian Ocean (Alexander et al. 1999). The ''reemergence mechanism'' explains rebounds in the North Pacific Ocean at a 12-month lead, arising after winter temperature anomalies in the deep-ocean mixed layer become separated from the surface because of stratification and resurface when the mixed layer deepens the following fall (Alexander et al. 1999). In this paper, we present evidence of a previously unidentified mechanism for rebound in predictability and show that this mechanism can play a significant role in atmospheric predictability.

2. The GLACE-2 forecast experiments and measures of potential predictability

The data used for this analysis come from the second phase of the Global Land–Atmosphere Coupling Experiment (GLACE-2), an internationally coordinated numerical modeling study in which ensembles of subseasonal forecasts are produced with a variety of state-of-the-art long-range forecasting systems (Koster et al. 2010, 2011). Each participating model produced two parallel sets of 2-month retrospective 10-member ensemble forecasts, with each forecast driven for a given start date by the same set of persisted sea surface temperature (SST) anomalies and starting with the same set of 10 slightly different atmospheric initial conditions (typically generated by perturbing the atmosphere). The key difference between the two forecast ensembles is that one set, denoted LA/O, is initialized with exactly the same ''realistic'' (observationally based) land surface conditions, whereas the other set, A/O, is initialized with ''randomized'' land surface conditions. For the latter set, the initial land state for each ensemble member is drawn from a probability density function appropriate for the forecast start date considered. Because the same atmospheric initial conditions and sea surface temperatures are used in the two sets of experiments, the comparison of predictability metrics between LA/O and A/O isolates the impact of land surface initialization on atmospheric predictability. Both sets of GLACE-2 experiments consist of 100 independent 2-month retrospective ensemble forecasts, one for each of 10 start dates (1 April, 15 April, . . . , 15 August) in each year spanning 1986–95. Forecasted precipitation, near-surface air temperature, soil moisture, and evaporation were averaged over four consecutive 15-day intervals for analysis.

A variable is defined to be unpredictable if its distribution given antecedent conditions is identical to the distribution regardless of antecedent conditions (Lorenz 1973). The former and latter distributions are called the forecast and climatological distributions, respectively. A necessary condition for predictability is for the forecast and climatological distributions to differ. A sufficient condition for distributions to differ is for the mean of one distribution to differ from the mean of another distribution. Thus, a test for predictability can be framed as a test of equality of means, for which the standard procedure is analysis of variance (ANOVA).

To quantify predictability, we note that the climatological variance can be partitioned into two parts: the variance of ensemble means and the variance about the ensemble mean. This partitioning can be expressed as

$$V_T = V_S + V_N, \tag{1}$$

$$\text{where} \quad V_T = \frac{1}{NE}\sum_{n=1}^{N}\sum_{e=1}^{E}(y_{en} - y_{\bullet\bullet})^2, \tag{2}$$

$$V_S = \frac{1}{N}\sum_{n=1}^{N}(y_{\bullet n} - y_{\bullet\bullet})^2, \quad \text{and} \tag{3}$$

$$V_N = \frac{1}{NE}\sum_{n=1}^{N}\sum_{e=1}^{E}(y_{en} - y_{\bullet n})^2. \tag{4}$$

Here, y_{en} denotes the forecast corresponding to antecedent condition n and the ensemble member e for that condition and $y_{\bullet\bullet} = 1/NE\sum_{n=1}^{N}\sum_{e=1}^{E}y_{en}$ and $y_{\bullet n} = 1/E\sum_{e=1}^{E}y_{en}$. Here, V_T, V_S, and V_N are called the total, signal, and noise variances, respectively. If the variable is unpredictable, the forecast means do not vary with antecedent conditions and hence have zero variance, implying $V_S \approx 0$. Moreover, (1) implies that the maximum of V_S is V_T. These considerations suggest that a natural measure of predictability is the signal-to-total ratio,

$$\text{STR} = \frac{V_S}{V_T}. \tag{5}$$

The STR is a measure of predictability in the sense that values near zero (one) indicate little or no (nearly maximum) predictability. Specifically, testing the significance of equality of means in ANOVA is equivalent to testing the significance of STR, because the two have identical information content.

In addition to measuring predictability, we also are interested in measuring differences in predictability due

to different initializations. An important issue is whether the climatological variance depends on initialization. The climatological variance is the variance over all realizations that occur on a specified calendar day. If the climatological variance for LA/O and A/O differ significantly, then we conclude that the A/O initialization effectively creates a new climate. Unfortunately, the comparison of predictability when the climatological variance changes with initialization is problematic, because the forecast and climatological distributions change in ways that are too complicated to be characterized by a simple signal-to-noise ratio. Therefore, we perform an equality of variance test between LA/O and A/O and eliminate models whose climatological variances differ from each other more than expected at the 5% significance level.

Having screened out models with significantly different variances between LA/O and A/O, we assume the total variance for the two initializations are equal. In this case, the ratio of STRs for LA/O and A/O reduces to the signal-to-signal ratio (SSR) and using its logarithm we can measure changes in predictability,

$$\mathrm{SSR} = \log_{10}\frac{V_S^{\mathrm{LA/O}}}{V_S^{\mathrm{A/O}}}. \tag{6}$$

If the predictability is the same for LA/O and A/O, then SSR ≈ 0. Thus, a test for equality of STRs reduces to a test for equality of signal variances.

We focus here on North America, where land surface initialization makes significant contributions to the subseasonal forecast skill of precipitation and near-surface air temperature (Koster et al. 2010, 2011). Eleven forecasting systems participated in GLACE-2, but we exclude models with incomplete output diagnostics or with total variances that differ significantly between the LA/O and A/O cases over the region of our interests (delineated by the box in Fig. 1). Four models satisfied both criteria for acceptability: the Canadian Centre for Climate Modeling and Analysis (CanCM3; Scinocca et al. 2008), the Center for Ocean-Land-Atmosphere Studies GCM V3.2 (Misra et al. 2007), the National Aeronautics and Space Administration (NASA) Global Modeling and Assimilation Office Goddard Earth Observing System-5 (GEOS-5) system (Bacmeister et al. 2000), and European Centre for Medium-Range Weather Forecasts/Max Planck Institute Hamburg forecast system (Roeckner et al. 2003; Raddatz et al. 2007). We conduct a multimodel analysis to reveal the consensus characterization of predictability. Data from these models are pooled for STR and SSR calculations.

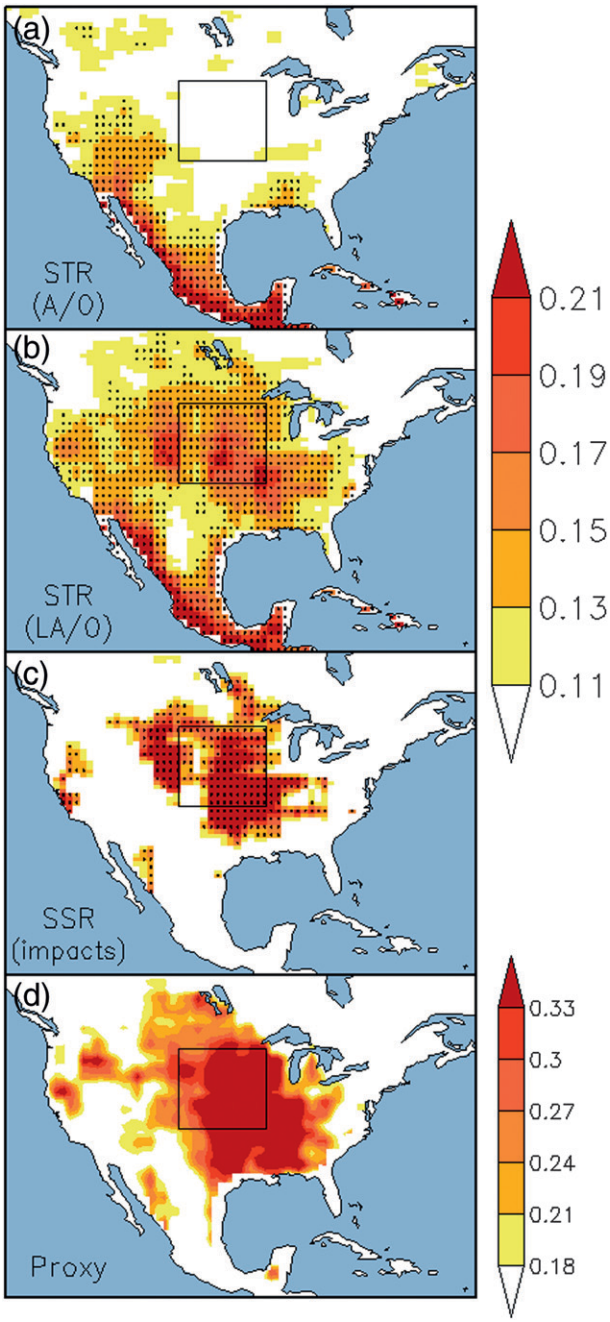

FIG. 1. (a),(b) The potential predictability (STR) for random (A/O) and realistic (LA/O) land surface initialization cases for the 46–60-day-average precipitation. (c),(d) Land surface impacts on potential predictability (SSR) for the 46–60-day-average precipitation and a proxy for soil moisture's contribution to land surface impacts on precipitation predictability. The dots show grid cells for which the measures are significant at the 5% significance level. Data from four of the models participating in GLACE-2 are used for the calculation.

3. Impacts of land surface on atmospheric potential predictability

Figure 1 shows the potential predictability (STR) of 46–60-day-average forecasted precipitation over North America for A/O and LA/O (top and second panels). All forecasts are used for the calculation. The dots indicate grid cells where the precipitation predictability is significant at the 95% confidence level. Precipitation has some predictability over the western United States and most of Mexico in the A/O case. By design, there is no predictability arising from land surface initialization, so the predictability is attributable to SST boundary forcing. The LA/O case exhibits significantly more predictability, especially over central North America. The SSR (third panel) isolates the influence of land initialization on potential predictability and confirms that predictability is significantly enhanced for the LA/O case over central North America.

At least two factors could contribute to this result: land–atmosphere coupling and soil moisture memory. Land–atmosphere coupling refers to processes that allow soil moisture variations to contribute to variations in the surface energy balance (e.g., latent and sensible heat fluxes), which in turn can affect the development of the atmospheric boundary layer and atmospheric variability. It can be quantified as the product of the standard deviation of evaporation and the correlation between soil moisture and evaporation anomalies (Guo et al. 2006; Dirmeyer et al. 2009). Soil moisture memory, measured by the lagged correlation of anomalies between the 1–15-day and 45–60-day forecast periods, quantifies the persistence of soil moisture anomalies. A proxy for soil moisture's contribution to atmospheric predictability is represented by the product of these two indices (here, the standard deviation and the correlations are calculated across the different years from the 15-day-average values). This proxy (bottom panel) has a geographic pattern similar to the SSR index, indicating that regions with strong land–atmosphere coupling and long soil moisture memory also have a significant impact on atmospheric predictability on the subseasonal time scale.

The region delineated by the box in Fig. 1 is chosen for detailed investigation of the temporal evolution of predictability. This area is selected because the predictability indices there are large and because it has recently experienced major droughts and floods (e.g., the drought of 1988 and the floods in 1993, 2008, and 2011). The areal averages of air temperature, precipitation, evaporation, and soil moisture are computed from the sequential 15-day averages for each ensemble member and start date. The top two panels of Fig. 2 show the predictability of air temperature and precipitation for LA/O (solid lines) and A/O (dashed lines). Each line represents results for forecasts starting at each of the 10 start dates from April through August.

A rapid drop in predictability is observed from the 1–15-day average to the 16–30-day average for both variables, indicating that the weather predictability from the atmospheric initialization dissipates rapidly. Even so, the predictability for LA/O is larger than for A/O in the 1–15-day averages, especially from June onward. This supports the previous finding that land surface initialization is also important for weather prediction, particularly during summer.

At each verification time, there are small variations in atmospheric predictability in the A/O case beyond the first 15 days. Meanwhile, there is a clear contrast in the evolution of atmospheric predictability between the random and realistic land surface initializations. Large dots indicate the intervals when the predictability in the LA/O case differs from that of the A/O case at the 95% confidence level. The differences in predictability between the A/O and LA/O cases are small during early to mid-spring and autumn, but significant from late spring through summer.

For the start dates in May and June, the predictability of precipitation and air temperature decreases in the first month and then increases sometime during the next 30–60 days; that is, the predictability rebounds in late spring and early summer. Figure 3 plots the STR change rates from days 16–30 to days 31–45 and from days 31–45 to days 46–60 for LA/O (open circles) and A/O (open triangles). The positive (negative) STR change rates indicate predictability rebound (decay). Positive STR change rates occur in the A/O case but most are statistically insignificant and are consistent with sampling fluctuations. Variations are largely symmetric about zero, suggesting that a spread of ± 0.1 approximates the range of random noise. The dotted lines in the plots indeed bound the central 90% of STR change rates for the A/O case. The figure shows that the change rates for LA/O are significantly larger than those for A/O and moreover exhibit a well-defined seasonal cycle, with large positive change rates occurring in May–July and large negative change rates occurring in early spring and late summer. In other words, the change rates for LA/O do not look random and look very different from A/O. The predictability rebound in the transition months from late spring to early summer show up prominently, as does the collapse of predictability during late summer and fall, when the strength of land–atmosphere coupling starts to decline. There are also large declines in early spring, because the effects of the land surface

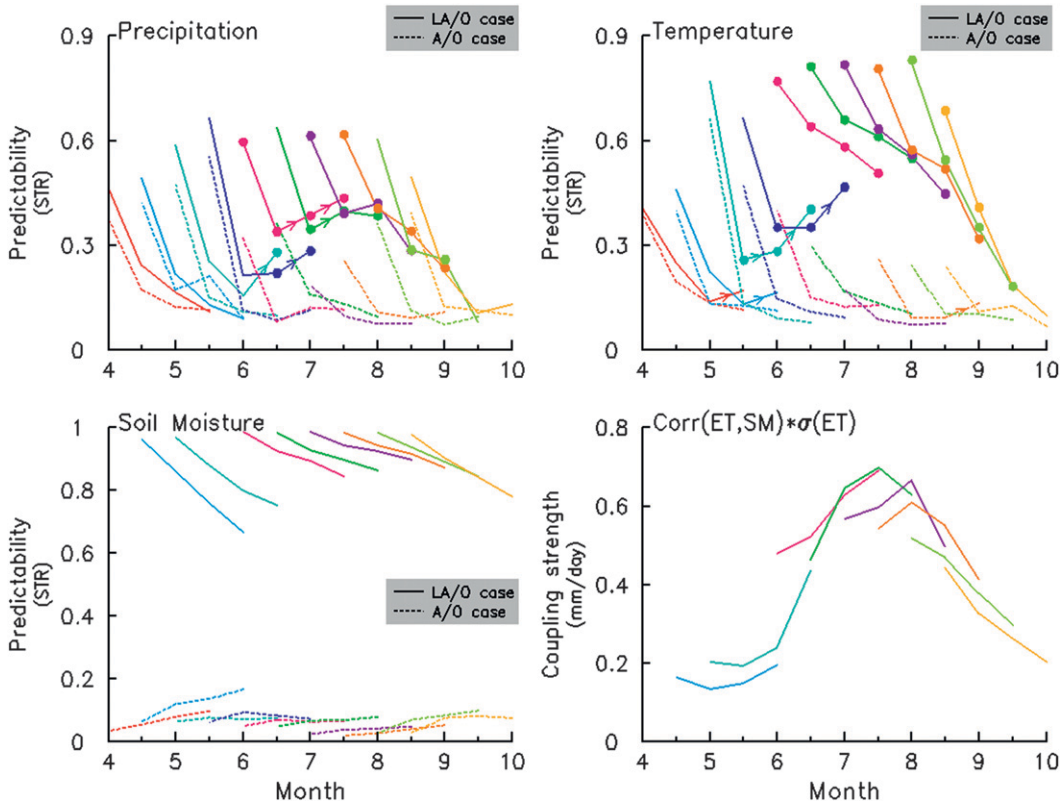

FIG. 2. Potential predictability (STR) of areal-average precipitation, near-surface air temperature, and soil moisture for random land surface initialization (A/O; dashed lines) and realistic land surface initialization (LA/O; solid lines), as well as land–atmosphere coupling strength computed as the product of the standard deviation of evaporation and the correlation between evaporation and soil moisture anomalies.

initialization on predictability at weather time scales (first 15 days) dissipate during days 16–30; in early spring, the mechanism for the rebound (see below) has not yet come into play. Among the 20 values of STR change rates for either variable in the LA/O case, the five largest rebounds occur within a narrow window during late spring and early summer. The likelihood that these five rebounds would randomly cluster in this confined period is less than 0.01%, and the magnitude of each of these five largest predictability rebounds is

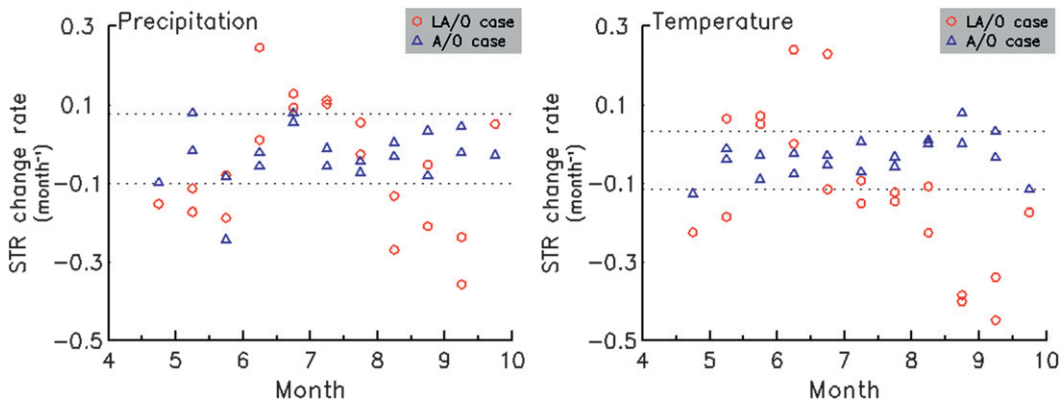

FIG. 3. Potential predictability (STR) change rates between adjacent periods for precipitation and near-surface air temperature in Fig. 2 with values for the first 15 days of each forecast period omitted.

statistically significant compared to the range of A/O examples.

4. Mechanism

The rebound in predictability is explained as a local transfer of information from the land surface to the atmosphere via physical processes that control the land–atmosphere coupling. The bottom panels of Fig. 2 showed the predictability of soil moisture and the land–atmosphere coupling strength index. As expected, soil moisture predictability with realistic land surface initialization is high for all periods because of the long persistence of soil moisture anomalies, and there is not a strong variation over time in this quantity. However, the coupling between the land and atmosphere exhibits a dramatic seasonal cycle: the coupling is weak in early spring, strengthens around mid-May, and peaks in mid-July, after which it gradually declines. Although soil moisture predictability remains high throughout, this predictability cannot influence the atmosphere in early spring because of weak land–atmosphere coupling. In essence, information in the land memory in spring is ''transferred'' to the atmosphere when coupling is established. Likewise, predictability declines in fall as coupling again weakens.

These results suggest that operational forecasts of subseasonal and seasonal rainfall and near-surface air temperature over North America during summer could be improved with information from antecedent soil moisture observations during spring. This would require monitoring of soil moisture anomalies in key regions and real-time availability of the observations to operational forecasting systems.

Acknowledgments. This research was supported by joint funding from the National Science Foundation (ATM-0830068), National Oceanic and Atmospheric Administration (NOAA; NA09OAR4310058), and the National Aeronautics and Space Administration (NASA; NNX09AN50G and NNX09AI84G) in the United States. We wish to thank all of the GLACE-2 participants. We also thank NOAA/MAPP and NASA Hydrology for their support of the overall coordination of the GLACE-2 project.

REFERENCES

Alexander, M. A., C. Deser, and M. S. Timlin, 1999: The re-emergence of SST anomalies in the North Pacific Ocean. *J. Climate,* **12,** 2419–2433.

Anderson, J. L., and H. M. Van den Dool, 1994: Skill and return of skill in dynamic extended-range forecasts. *Mon. Wea. Rev.,* **122,** 507–516.

Bacmeister, J., P. J. Pegion, S. D. Schubert, and M. J. Suarez, 2000: Atlas of seasonal means simulated by the NSIPP 1 atmospheric GCM. NASA Tech. Memo. 2000-104606, Vol. 17, 194 pp.

Cover, T. M., and J. A. Thomas, 1991: *Elements of Information Theory.* Wiley-Interscience, 542 pp.

DelSole, T., and M. K. Tippett, 2007: Predictability: Recent insights from information theory. *Rev. Geophys.,* **45,** RG4002, doi:10.1029/2006RG000202.

Dirmeyer, P. A., C. A. Schlosser, and K. L. Brubaker, 2009: Precipitation, recycling and land memory: An integrated analysis. *J. Hydrometeor.,* **10,** 278–288.

Guo, Z., and Coauthors, 2006: GLACE: The Global Land–Atmosphere Coupling Experiment. Part II: Analysis. *J. Hydrometeor.,* **7,** 611–625.

Kleeman, R., 2007: Information flow in ensemble weather predictions. *J. Atmos. Sci.,* **64,** 1005–1016.

Koster, R. D., and Coauthors, 2010: Contribution of land surface initialization to subseasonal forecast skill: First results from a multi-model experiment. *Geophys. Res. Lett.,* **37,** L02402, doi:10.1029/2009GL041677.

——, and Coauthors, 2011: The second phase of the Global Land–Atmosphere Coupling Experiment: Soil moisture contributions to subseasonal forecast skill. *J. Hydrometeor.,* **12,** 805–822.

Lorenz, E. N., 1973: Predictability and periodicity: A review and extension. *Proc. Third Conf. on Predictability and Statistics in the Atmospheric Sciences,* Boulder, CO, Amer. Meteor. Soc., 1–4.

Misra, V., and Coauthors, 2007: Validating and understanding ENSO simulation in two coupled climate models. *Tellus,* **59A,** 292–308.

Philander, S. G. H., 1990: *El Niño, La Niña, and the Southern Oscillation.* Academic Press, 293 pp.

Raddatz, T. J., and Coauthors, 2007: Will the tropical land biosphere dominate the climate–carbon cycle feedback during the twenty-first century? *Climate Dyn.,* **29,** 565–574, doi:10.1007/s00382-007-0247-8.

Roeckner, E., and Coauthors, 2003: The atmospheric general circulation model ECHAM5. Part I: Model description. Max-Planck-Institute for Meteorology Rep. 349, 140 pp.

Scinocca, J. F., N. A. McFarlane, M. Lazare, J. Li, and D. Plummer, 2008: The CCCma third generation AGCM and its extension into the middle atmosphere. *Atmos. Chem. Phys.,* **8,** 7055–7074.

Shukla, J., 1981: Dynamical predictability of monthly means. *J. Atmos. Sci.,* **38,** 2547–2572.

——, and J. L. Kinter, 2006: Predictability of seasonal climate variations: A pedagogical view. *Predictability of Weather and Climate,* T. N. Palmer and R. Hagedorn, Eds., Cambridge University Press, 306–341.

Simmons, A. J., and A. Hollingsworth, 2002: Some aspects of the improvement in skill of numerical weather prediction. *Quart. J. Roy. Meteor. Soc.,* **128,** 647–677.

Wajsowicz, R. C., 2007: Seasonal-to-interannual forecasting of tropical Indian Ocean sea surface temperature anomalies: Potential predictability and barriers. *J. Climate,* **20,** 3320–3343.